The Role of Protein Dynamics in Increasing Binding Affinity for an Engineered Protein−Protein Interaction Established by H/D Exchange Mass Spectrometry[†]

James R. Horn,[‡,⊥] Brian Kraybill,[§,⊥] Elizabeth J. Petro,[‡] Stephen J. Coales,[§] Jeffrey A. Morrow,[#] Yoshitomo Hamuro,[§] and Anthony A. Kossiakoff*[,‡,||]

Department of Biochemistry and Molecular Biology, and Institute for Biophysical Dynamics, Center for Integrative Science, The University of Chicago, 929 East 57th Street, Chicago, Illinois 60637, ExSAR Corporation, 11 Deer Park Drive, Suite 103, Monmouth Junction, New Jersey 08852, and Sierra Analytics, Inc., 5815 Stoddard Road, Suite 601, Modesto, California 95356

Received March 3, 2006; Revised Manuscript Received May 17, 2006

ABSTRACT: It is generally accepted that protein and solvation dynamics play fundamental roles in the mechanisms of protein−protein binding; however, assessing their contribution meaningfully has not been straightforward. Here, hydrogen/deuterium exchange mass spectrometry (H/D-Ex) was employed to assess the role of dynamics for a high-affinity human growth hormone variant (hGHv) and the wild-type growth hormone (wt-hGH) each binding to the extracellular domain of their receptor (hGHbp). Comparative analysis of the transient fluctuations in the bound and unbound states revealed that helix-1 of hGHv undergoes significant transient unfolding in its unbound state, a characteristic that was not found in wt-hGH or apparent in the temperature factor data from the X-ray analysis of the unbound hGHv structure. In addition, upon hormone binding, an overall increase in stability was observed for the β-sheet structure of hGHbp which included sites distant from the binding interface. On the basis of the stability, binding kinetics, and thermodynamic data presented, the increase in the binding free energy of hGHv is primarily generated by factors that appear to increase the energy of the unbound state relative to the free energy of the bound complex. This implies that an alternate route to engineer new interactions aiming to increase protein−protein association energies may be achieved by introducing certain mutations that destabilize one of the interacting molecules without destabilizing the resulting bound complex. Importantly, although the hGHv molecule is less stable than its wt-hGH counterpart, its resulting active ternary complex with two copies of hGHbp has comparable stability to the wt complex.

A principal goal in structural biophysics is to develop general rules for structure−function relationships that govern protein−protein interactions, ultimately to quantify the contribution of individual local interactions to the overall binding energy. In this regard, there is a growing appreciation that essentially all interactions are context-dependent, and factors such as solvation and dynamics play critical, if not dominant, roles in forming most surface-to-surface contacts. Because solvation and dynamics are inherently difficult phenomena to quantify experimentally, their influence many times is invoked in a very general way, especially when structure-based rationales fail to explain biophysical data.

The interaction between a high-affinity variant of human growth hormone (hGH) and the extracellular domain of its cognate receptor (hGHbp)[1] represents one of the cases where the binding properties are difficult to rationalize based on general structure−function principals. This variant (hGHv) was produced by phage display mutagenesis and binds through Site-1 to hGHbp with a K_d < 10 pM, which constitutes a ∼400-fold (∼3 kcal/mol) increased affinity over the wild-type hormone (wt-hGH), K_d ∼1 nM (*1*−*3*). It contains 15 mutations in its Site-1 binding interface and retains its full biological activity (*4*).

An unanticipated finding was that a surprisingly large fraction of the mutations in hGHv was stereochemically improbable based on the structural interactions in the wt-hGH complex (*5*). The mutagenesis produced a systematic conversion of hydrophilic to hydrophobic side chains. For instance, a number of hydrophilic side chains that were involved in H-bonds or salt-bridges with complementary hydrophilic groups in hGHbp were converted to hydrophobic residues. This resulted in a completely altered H-bonding network between the hormone and hGHbp and a somewhat more hydrophobic interface.

The fact that the differences in the binding properties between wt-hGH and hGHv involve a complex mix of factors is apparent when their functional epitopes are compared. The total binding interface of wt-hGH consists of ∼35 residues;

[†] This work was supported by a grant from the National Institutes for Health (DK-61602) to A.A.K. J.R.H. was supported by a postdoctoral fellowship from the American Heart Association.

* To whom correspondence should be addressed. Phone, (773) 702-9257; fax, (773) 834-2777; e-mail, koss@cummings.uchicago.edu.

[‡] Department of Biochemistry and Molecular Biology, The University of Chicago.

[⊥] These authors contributed equally to this work.

[§] ExSAR Corporation.

[#] Sierra Analytics, Inc.

[||] Institute for Biophysical Dynamics, Center for Integrative Science, The University of Chicago.

[1] Abbreviations: H/D-Ex, hydrogen/deuterium exchange; wt-hGH, wild-type human growth hormone; hGHv, phage display optimized human growth hormone variant; hGHbp, human growth hormone binding protein (receptor).

10.1021/bi0604328 CCC: $33.50
Published on Web 06/22/2006

however, its functional epitope is considerably smaller and is characterized by a defined hot-spot, where much of the binding energy is concentrated among contributions from 7 to 8 side chains (*6*−*8*). In contrast, even though it binds with significantly higher affinity, hGHv does not have a similar hot-spot (*9*). The binding contributions of the comparable hot-spot residues found in wt-hGH are highly attenuated in hGHv. Interestingly, some of these groups have identical packing environments and make virtually identical interactions in both cases, but in the context of their parent molecules, they produce dramatically different effects. Furthermore, the new set of H-bonds and van der Waals interactions in hGHv provide little new additional binding energy to the interaction (*9*).

Another distinguishing trait of the hGHv−hGHbp Site-1 interface is the distribution of enthalpic (ΔH) and entropic (ΔS) contributions to the binding thermodynamics (*3*). In the wt-hGH case, binding to hGHbp is characterized by favorable contributions from both ΔH and ΔS factors. In contrast, for hGHv, the partitioning of the ΔH and ΔS contributions is radically different. The ΔG for binding is generated from a much more favorable ΔH term, counterbalanced by an extremely unfavorable $T\Delta S$ component. While it is known that binding induces a significant structural organization of both the hormone and receptor molecules, the extent of this reorganization is most likely similar for the wt-hGH and hGHv cases based on crystal structure evidence (*5*). Thus, it is hard to imagine the large disparity in the entropic component in these systems can be ascribed simply to differences related to freezing out more configurational degrees of freedom in hGHv. Likewise, the large differences in enthalpy cannot merely be due to a more potent set of H-bonding and van der Waals interactions in hGHv. Furthermore, the observed thermodynamic profile is counterintuitive of what is predicted based on empirical, structure-derived relationships (*10*), where a more hydrophobic interface favors a more favorable ΔS and less favorable ΔH.

On the basis of the combination of the above observations, it was clear to us that some underlying features of the systems cannot be understood by relating the biochemical/biophysical data to the time-averaged structures of the unbound and bound molecules. An obvious missing component in this analysis was the contributions due to differences in the dynamic behavior of the hGHv compared to wt-hGH, in either the unbound or bound states, or both. Thus, our premise was that the energetics resulting from the interplay between structure and dynamics is a major determinant in the hGHv−hGHbp binding mechanism and that this mechanism could be fundamentally different from the one that drives the wt-hGH−hGHbp association.

As the structure−function relationships based only on time-averaged structures are inadequate, a major challenge was to acquire experimental data that captured the relevant structure-dynamics relationships in the hGHv−hGHbp binding mechanism. In this regard, the hydrogen/deuterium exchange technique (H/D-Ex) is particularly powerful through its ability to identify transient fluctuations in protein molecules or protein−protein interfaces (*11*−*13*). This is because the rate of exchange of a backbone amide hydrogen in the interior of a protein molecule is a direct function of the energy required to distort the polypeptide chain to provide access to the deuterated solvent. Indeed, the H-to-D exchange rates of interior sites are found to differ by several orders of magnitude in an intact protein, providing a sensitive measure of protein secondary and tertiary stability (*14*). Protein shielding can also be detected when stability changes are modest. H/D exchange also has advantages over other labeling techniques in that a deuteron has a negligible space requirement and has nearly equivalent chemical properties to the proton it replaces in the structure. Furthermore, labile sites are distributed fairly uniformly throughout the molecule and therefore probe the structural plasticity of the whole molecule.

However, as potentially powerful as the H/D-Ex method is in determining the dynamic profile of a protein's structure, it remains a somewhat underutilized approach. NMR provides the most straightforward approach to extract high-resolution H/D exchange information, especially for smaller proteins (*11*). Neutron diffraction studies have also established that high-resolution H/D exchange patterns can be determined from a time-averaged analysis (*12*), but the technique is fraught with experimental barriers (*14*). More recently, mass spectrometry methods have been developed and employed to accurately determine H/D exchange patterns for proteins (*15*−*20*), protein−small molecule complexes (*13*, *21*, *22*), and protein−protein complexes (*23*−*25*). While this method does not have the single-residue resolution of NMR, it is has the advantage of speed and the ability to analyze larger proteins and protein complexes.

On the basis of its ability to link dynamics to structure, we have used H/D exchange coupled with mass spectrometry (H/D-Ex) to probe the spatial distribution of transient fluctuations in hGHv, wt-hGH, hGHbp, and their respective complexes. We were interested in determining whether wt-hGH and hGHv have different dynamical behaviors when comparing their unbound and bound states. If so, how different are they and where do the differences occur in the molecules?

Using the H/D-Ex method, we identified distinct differences in the dynamic properties of the unbound states of wt-hGH and hGHv. These data suggest that the unbound hGHv molecule undergoes a significant degree of transient "regional melting," particularly involving the secondary structure of helix-1, and that its binding to the receptor (hGHbp) involves a local disorder to order transition. These characteristics are not emulated during formation of the wt-hGH/hGHbp complex. Coupling the H/D-Ex data with the thermodynamic binding data allowed us to establish that the binding mechanisms of wt-hGH and hGHv are fundamentally different. The binding mechanism for hGHv also helps explain the "loss" of the hot-spot in hGHv and can explain why such a mechanism cannot be recognized by examining Ala scanning data alone.

We note that the hGHv molecule described here is now in clinical use for the treatment of acromegaly.

MATERIALS AND METHODS

Protein Expression and Purification. The wt-hGH and hGHv were expressed and purified as described previously (*26*). The extracellular domain of hGHbp (residues 29−238) was expressed and purified as described (*27*) with the exception that hGHbp is eluted with 4.5 M $MgCl_2$.

H/D Exchange: Stock Solutions for H/D-Ex of wt-hGH and hGHv with hGHbp. A stock solution for H/D-Ex was

prepared by mixing 31.1 μL of wt-hGH solution (61 μM) and 68.9 μL of hGHbp (33 μM). When the H/D-Ex pattern of wt-hGH was followed, 1.2 mol excess of hGHbp was mixed with wt-hGH to ensure all wt-hGH was in the complex with hGHbp. The dissociation constant for wt-hGH/hGHbp is $K_d \sim 1$ nM (*2*). For the control experiment, the hGHbp solution was replaced by a 10 mM Tris and 150 mM NaCl, pH 7.5, buffer. For the experiments of hGHv, a slightly different ratio of the protein solutions was used (33.8 μL of 53.5 μM hGHv solution and 66.2 μL of 33 μM hGHbp solution) to keep the same 1.2 mol excess of hGHbp over hGHv. The dissociation constant for the hGHv/hGHbp complex is $K_d < 10$ pM (*2*). Volumes of 10 μL of stock solution and 10 μL of deuterated buffer were mixed to initiate the exchange reaction. The final concentration of hGH and hGHv used in the exchange solutions were 9.5 and 9.1 μM, respectively.

Stock Solutions for H/D-EX of hGHbp Alone and in the Presence of wt-hGH or hGHv. A stock solution for H/D-EX was prepared by mixing 39.4 μL of wt-hGH solution (61 μM) and 60.6 μL of hGHbp (33 μM). When the H/D-EX pattern of hGHbp was followed, 1.2 mol excess of wt-hGH was mixed with hGHbp to ensure all hGHbp was in the complex with wt-hGH. For the control experiment, the wt-hGH solution was replaced by a 10 mM Tris and 150 mM NaCl, pH 7.5, buffer. For the experiments with hGHv, a slightly different ratio of the protein solutions was used (42.4 μL of 53.5 μM hGHv solution and 57.6 μL of 33 μM hGHbp solution) to keep the same 1.2 mol excess of hGHbp over hGHv. After 10 uL of stock solution was mixed with 10 μL of deuterated buffer, the final concentration of hGHbp was 10.0 and 9.5 μM for the hGH and hGH SM experiments, respectively.

Hydrogen/Deuterium Exchange Experiments. An hGH−hGHbp stock solution was prepared in the aforementioned manner. An exchange reaction was initiated by diluting 10 μL of a stock solution (± binding partner) with 10 μL of deuterated buffer (25 mM Tris and 150 mM NaCl, pH 7.5). The reaction mixture was incubated at 25 ± 1 °C for varying durations (30−10 000 s). These functionally deuterated samples were then subjected to H/D-EX analysis as below, along with control samples of nondeuterated and fully deuterated protein (incubated in 50 mM TCEP in 50% D_2O for 1 day at 60 °C).

General Operation Procedure. A 20 μL H/D-exchanged protein solution was quenched by shifting to pH 2.5, 0 °C, with 30 μL of 8 M urea and 1 M TCEP. At 1 °C, the quenched solution was immediately passed over a pepsin column (104 μL of bed volume) filled with porcine pepsin (Sigma) immobilized on Poros 20 AL media at 30 mg/mL per the manufacturer's instructions, with 0.05% TFA (200 μL/min) for 3 min with contemporaneous collection of proteolytic products by a trap column. Subsequently, the peptide fragments were eluted from the trap column and separated by C18 column (Magic C18, Michrom BioResources, Inc, Auburn, CA) with a linear gradient of 13%−40% B over 23 min (solvent A, 0.05% TFA in water; solvent B, 95% acetonitrile, 20% water, 0.01% TFA; flow rate 5−10 μL/min). Mass spectrometric analyses were carried out with a Thermo Finnigan LCQ mass spectrometer (Thermo Electron Corporation, San Jose, CA) with capillary temperature at 200 °C.

Sequence Identification of Pepsin-Generated Peptides. To quickly identify pepsin-generated peptides for each digestion condition employed, spectral data was acquired in data-dependent MS/MS mode with dynamic exclusion. Sequest software program (Thermo Electron Corporation) was used to identify the sequence of the dynamically selected parent peptide ions. This tentative peptide identification was verified by visual confirmation of the parent ion charge state presumed by the Sequest program for each peptide. This set of peptides was then further examined to determine if the 'quality' of the measured isotopic envelope of peptides was sufficient to allow accurate measurement of the geometric centroid of isotopic envelopes on deuterated samples.

Calculation of Deuteration Level. The centroids of probe peptide isotopic envelopes were measured using the in-house-developed program in collaboration with Sierra Analytics. The corrections for back-exchange were made employing methods described previously (*15*, *16*).

$$\textit{Deuteration Level}\ (\%) = \frac{m(\mathrm{P}) - m(\mathrm{N})}{m(\mathrm{F}) - m(\mathrm{N})} \times 100 \quad (1)$$

$$\textit{Deuteration Incorporation}\ (\mathrm{no.}) = \frac{m(\mathrm{P}) - m(\mathrm{N})}{m(\mathrm{F}) - m(\mathrm{N})} \times \mathrm{MaxD} \quad (2)$$

where m(P), m(N), and m(F) are the centroid value of partially deuterated peptide, nondeuterated peptide, and fully deuterated peptide, respectively. MaxD is the maximum deuterium incorporation calculated by subtracting the number of prolines in the third or later amino acid and two from the number of amino acids in the peptide of interest (assuming the first two amino acids cannot retain deuterons. The deuteron recovery of fully deuterated sample ((m(F) − m(N))/MaxD) was on average 65% for hGHbp and 71% for wt-hGH and hGHv.

Circular Dichroism. All CD experiments were performed on an Aviv Instruments circular dichroism spectrometer model 202 equipped with a Hamilton Microlab 500 series titrator. CD scans were performed at 25°C from 260−200 nm in PBS (10 mM NaPhosphate, 150 mM NaCl, pH 7.4) using a 1 cm path length quartz cuvette. For guanidine denaturation experiments, 0.8 μM hormone was prepared in both PBS buffer and PBS/7 M guanidine-hydrochloride. Chemical melts were automatically titrated injecting protein in PBS buffer containing 7 M guanidine-hydrochloride PBS into the stirred cuvette containing the protein in PBS. Data were analyzed using the program Sigma Plot Enzyme Kinetics Module. Unfolding curves were fit to a two-state unfolding equilibrium. All errors are ± 1 standard deviation and originate from the fitting program.

Calculations. Surface area calculations were performed using the program NACCESS (*28*).

RESULTS

H/D Exchange: Proteolytic Fragmentations and Sequence Coverage of wt-hGH, hGHv, and hGHbp. Prior to H/D exchange experiments, digestion conditions that produced protein fragments of optimal size and distribution for exchange analysis were established (see Materials and

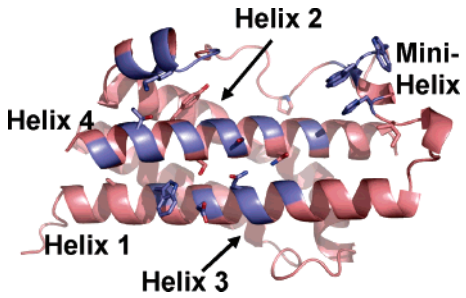

FIGURE 1: Ribbon representation of hGHv. The 15 substituted residues are shown in stick format. These include residues F10A, M14W, H18D, H21N, K41I, Y42H, L45W, Q46W, F54P, R64K, R167N, D171S, E174S, F176Y, and I179T. Helices 1−4 are indicated on the figure. The interface residues are highlighted in blue.

Methods). Pepsin digestion of each protein was carried out by diluting the deuterated sample (1:1) with cold quench solution (8 M urea, 1 M TCEP, pH 2.5). The quenched sample was then flowed over immobilized pepsin (104 μL bed volume) at a flow rate of 200 μL/min at 1 °C, allowing a digest time of 31 s. The condition gave 93% (= 177/191) sequence coverage for wt-hGH, 88% (= 168/191) for hGHv, and 100% (= 210/210) for hGHbp (see Supplementary Figure 1, Supporting Information, for peptide map).

Since both the amino group of the first amino acid and the amide hydrogen of the second amino acid tend to exchange too rapidly to retain deuterons during the experiment, there is a two residue gap between two peptides in the following H/D exchange results (for example, peptide 10−15 gave H/D exchange results of residues 12−15). It is interesting to note that despite many mutations in hGHv, the digestion patterns of wt-hGH and hGHv were very similar, except for one residue shift near the N-terminus.

Overall, the H/D exchange data appear to represent accurately what is expected based on existing crystal structure data of the hGH/hGHbp and hGHv/hGHbp complexes (*5*) and NMR data on wt-hGH (*29*) (Figure 1). Figure 2 demonstrates the normalized raw data for a small subset of peptides and displays their relationship to the hGH structure when allowed to exchange with and without the presence of hGHbp. This example illustrates the dynamic range of exchange that can be defined with this technique. There are regions that are solvent-exposed and show complete exchange in the dead time of data acquisition with and without hGHbp (Figure 2, section A), and regions buried in the interface that become more protected (to various degrees) in the presence of hGHbp (Figure 2, sections B and C). There are also regions that are buried and/or have all exchangeable amide protons involved in H-bonds and consequently do not exchange in the 10 000 s time span with or without hGHbp present (e.g., Figure 2, section D). The entire set of normalized data is available in Supplementary Figures 2−5 (Supporting Information).

H/D Exchange of Unbound wt-hGH and hGHv. The H/D exchange patterns for wt-hGH and hGHv indicate that these molecules have similar modes of flexibility/solvent accessibility in their unbound states with the exception of helix-1 and to a lesser extent helix-4 (Figure 3a/Supplementary Figure 4, Supporting Information). Helix-1 is a 29 residue α-helix (residues 6−35) that is probed by H/D-Ex using three peptides: 12−15, 18−25, and 28−31. Helix-4 is a 26 residue

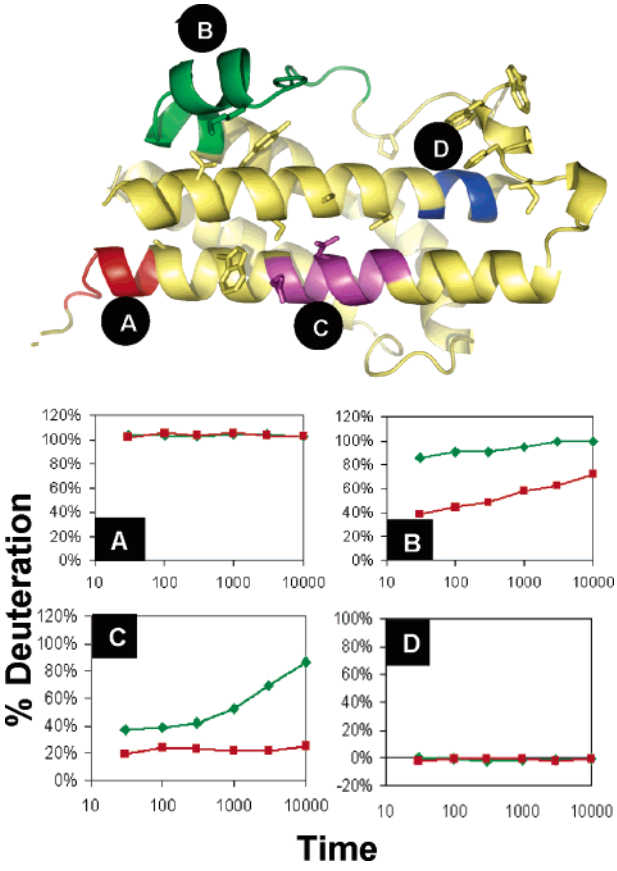

FIGURE 2: Ribbon diagram of hGH highlighted by four different regions that are reported in the H/D-EX data. These include residues 3−9 (A) where complete exchange occurs in the dead time of data acquisition, regions including residues 18−25 (B) and 56−75 (C) in the interface which becomes protected to various degrees upon binding the hGHbp, and regions 160−163 (D) whose amide nitrogens are buried/involved in hydrogen bonds and do not exchange in either unbound or bound state. All protein structure figures were generated with the program PYMOL(*48*).

α-helix (residue 157−183) that is described by three peptides: 160−163, 166−176, and 179−191. Helix-2 is characterized by very slow exchange (Table 1/Supplemetary Figure 4, Supporting Information). Helix-3 could not be resolved for technical reasons. Overall, helix-1 displays somewhat more flexibility in wt-hGH than the other two helices, but most of this is concentrated in the N-terminal end (preceding residue 18). In the case of hGHv, however, all sections of helix-1 display a pronounced increase (∼25%) in the extent of exchange over the wild-type molecule, and helix-4 possesses two regions on the C-terminal end that display somewhat enhanced exchange (∼13%) (Figure 3a).

H/D Exchange of wt-hGH and hGHv with or without hGHbp. The H/D exchange patterns of wt-hGH and hGHv with or without hGHbp are presented in Table 1. As expected, a decrease in exchange was observed for regions known to participate in the hormone/receptor interface (Figure 4). Several segments of hGHv showed significantly greater protection upon hGHbp binding compared with wt-hGH; 18−25, 28−31, 33−44, and 56−75 and another with marginal increase in protection at residues 95−97, the C-terminal of hGHv (residues 179−191) (Table 1/ Figure 4b). Among these segments, the higher degree of protection at 18−25 and 28−33 and the marginal protection at 95−97 and 179−191 is presumably due to the destabilization of free

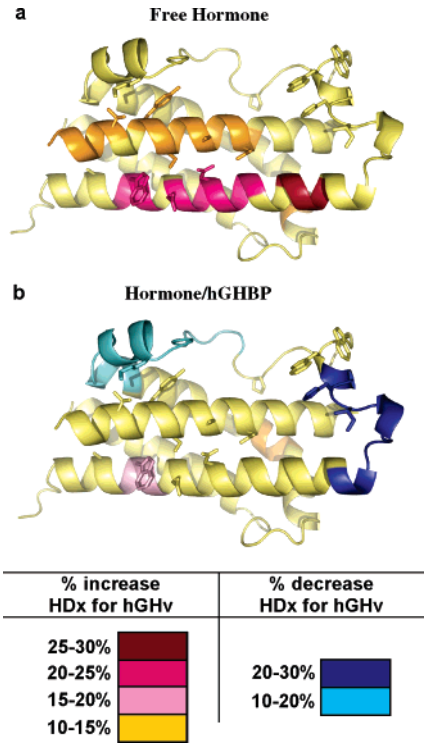

FIGURE 3: Ribbon diagram of hGHv displaying increases in H/D exchange between the free hormones hGH and hGHv (a) and the hormone/receptor complexes wt-hGH/hGHbp and hGHv/hGHbp (b). Degree of exchange is color-coded according to legend.

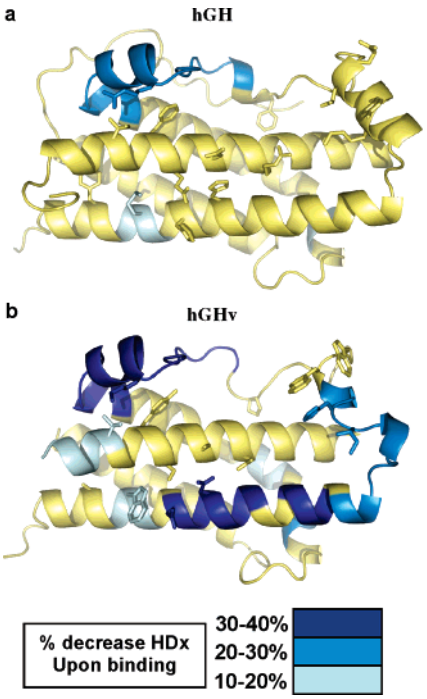

FIGURE 4: Ribbon diagram illustrating the percent decrease in H/D exchange upon binding for wt-hGH (a) and hGHv (b). Percent increase in exchange is color-coded according to legend.

Table 1: Average Difference in Deutertion Level[a]

residues	wt-hGH ± BP	hGHv ± BP	hGHv−wt-hGH	hGHv/BP −wt-hGH/BP
3−9 (+1)	−5%	0%	3%	8%
12−15 (+1)	−12%	−19%	23%	17%
18−25 (+2)	−6%	−32%	21%	−5%
28−31 (+1)	−5%	−33%	29%	1%
33−44 (+2)	−4%	−28%	3%	−21%
47−53 (+1)	−1%	n/a	n/a	n/a
56−75 (+2)	−29%	−39%	−1%	−11%
78−80 (+1)	−1%	−2%	0%	−1%
83−85 (+1)	1%	−4%	5%	0%
88−92 (+1)	−10%	−5%	9%	14%
95−97 (+1)	−12%	−20%	10%	3%
100−110 (+1)	−1%	0%	2%	3%
127−146 (+3)	5%	4%	0%	0%
149−157 (+1)	1%	4%	1%	4%
160−163 (+1)	1%	0%	1%	0%
166−176 (+2)	1%	−5%	14%	8%
179−191 (+2)	−6%	−12%	11%	5%

[a] wt-hGH ± BP means the average difference in deuteration between wt-hGH alone and wt-hGH in the presence of hGHbp. The differences at all six time points in each segment were averaged. A negative number indicates exchange was slower in the presence of hGHbp. hGHv ± BP means the average difference in deuteration between hGHv alone and hGHv in the presence of hGHbp. A negative number indicates exchange was slower in the presence of hGHbp. hGHv−wt-hGH means the average difference in deuteration between wt-hGH alone and hGHv alone. A positive number indicates that exchange was faster in hGHv. hGHv/BP−wt-hGH/BP means the average difference in deuteration between hGHv with hGHbp and wt-hGH with hGHbp. A positive number indicates exchange was faster in hGHv with hGHbp.

hGHv, as evidenced by the faster exchange in free hGHv than free wt-hGH (Figure 3a). On the other hand, the greater protection at 33−44 and 56−75 results from a more a stable hGHv−hGHbp complex formation, a model consistent with the slower exchange in hGHv−hGHbp than in wt-hGH−hGHbp.

H/D Exchange of hGHbp Alone and in the Presence of wt-hGH or hGHv. The H/D exchange patterns of unbound hGHbp and those in the presence of wt-hGH or hGHv were determined and are presented in Table 2 and Figure 5. The hGHbp regions that showed increased protection in wt-hGH and hGHv complexes were very similar (Figure 5a,b). There are several regions where hGHv retards the H/D exchange of hGHbp compared to wt-hGH, such as 103−108, 123−126, and 167−172 (Figure 5c). The diminished rate of exchange in these regions is likely due to the slower dissociation rate of hGHv, since these regions are buried in the hGHv/hGHbp interface. It is noteworthy that the regions of significant protection from exchange upon hormone binding are not limited to the protein−protein interface. For instance, there are regions that extend from the interface into regions in the C-terminal domain (e.g., 154−164, 210−225), while there are also regions that are completely removed from any contact with the interface (e.g., 175−177, 196−202, 203−207, and 228−230) (Figure 5d).

Circular Dichroism and Chemical Stability. The far-UV CD spectra of hGH and hGHv were obtained (Figure 6a). Both proteins exhibit a double minimum near 222 and 208 nm, a strong characteristic of four-helix bundle proteins which is also supported by crystallographic data of hGH and hGHv (*30*). There is no discernible difference in the spectra, within instrument error, between these two hormones. This suggests that the solution state "average" secondary structure is very similar between hGH and hGHv.

To test how the 15 amino acid surface substitutions within hGHv affect intramolecular interactions, guanidine chemical denaturation experiments were performed (Figure 6b). The stability for hGH and hGHv were 11.58 ± 0.02 and 8.00 ± 0.01 kcal/mol, respectively, representing a ~3.5 kcal/mol

Table 2: Average Difference in Deutertion Level[a]

residues	BP ± wt-hGH	BP ± hGHv	hGHbp/hGHv−hGHbp/wt-hGH
31−48 (+2)	−45%	−49%	−5%
51−66 (+2)	−10%	−10%	1%
69−75 (+1)	−12%	−11%	1%
76−79 (+)	0%	4%	3%
82−94 (+1)	−29%	−31%	−1%
97−100 (+1)	−28%	−32%	−4%
103−108 (+1)	−28%	−42%	−14%
111−122 (+2)	−24%	−21%	3%
123−126 (+)	−58%	−89%	−31%
129−138 (+1)	−38%	−43%	−4%
140−142 (+1)	−9%	−5%	3%
145−151 (+1)	6%	10%	4%
154−164 (+2)	−41%	−34%	8%
167−172 (+1)	−35%	−69%	−34%
175−177 (+1)	−12%	−13%	−1%
180−193 (+2)	−8%	−12%	−4%
196−202 (+1)	−30%	−32%	−2%
203−207 (+)	−35%	−32%	2%
210−225 (+3)	−21%	−31%	−10%
228−230 (+1)	−15%	−13%	2%
233−238 (+1)	−6%	−2%	4%

[a] BP ± wt-hGH means the average difference in deuteration between hGHbp alone and hGHbp in the presence of wt-hGH. A negative number indicates exchange was slower in the presence of wt-hGH. BP ± hGHv means the average difference in deuteration between hGHbp alone and hGHbp in the presence of hGHv. A negative number indicates exchange was slower in the presence of hGHv. hGHbp/hGHv−hGHbp/wt-hGH means the average difference in deuteration between hGHbp with hGHv and hGHbp with wt-hGH. A negative number indicates exchange was slower in the presence of hGHv.

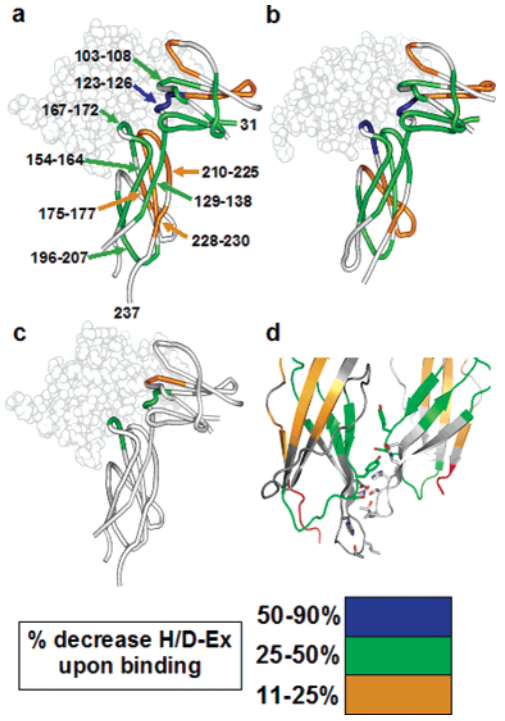

FIGURE 5: Ribbon diagram of hGHbp illustrating the percent decrease in exchange in hGHbp upon binding wt-hGH (a) and hGHv (b) and their difference (c). (d) Ribbon diagram highlighting the receptor−receptor contact region with those residues involved in intermolecular interactions displayed in stick format.

decrease in stability. The *m*-values for wt-hGH and hGHv were 2520 ± 40 and 2040 ± 40 kcal/mol urea, respectively. A decrease in *m*-values is typically correlated with less surface area exposure upon unfolding (*31*).

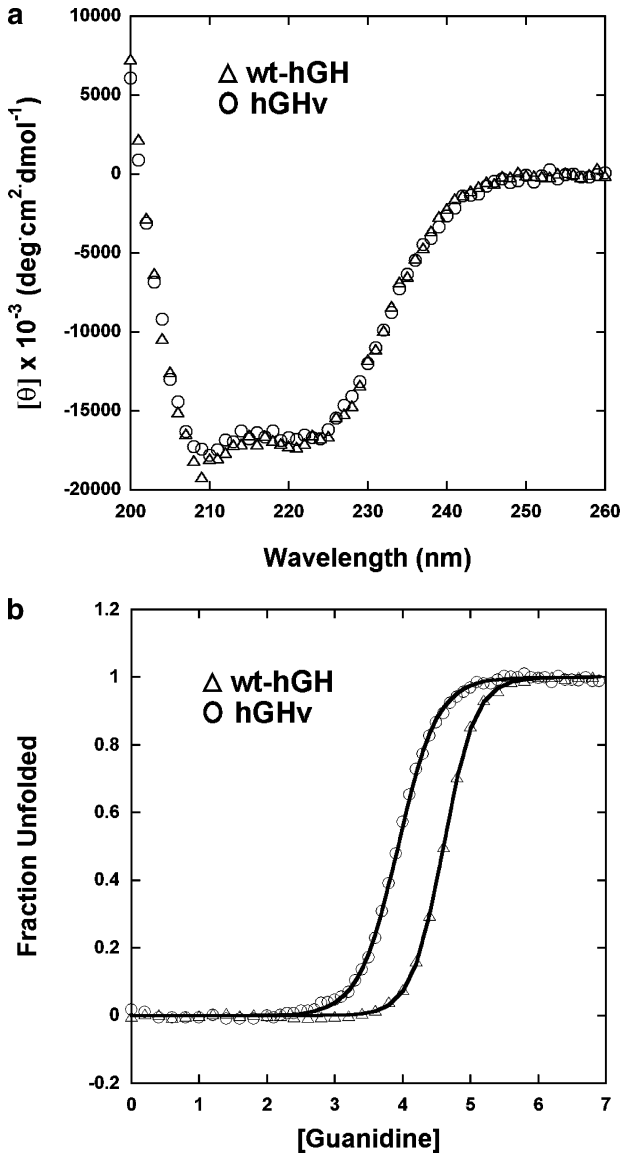

FIGURE 6: (a) Far-UV circular dichroism scan of wt-hGH and hGHv. (b) Guanidine unfolding curves of wt-hGH and hGHv.

DISCUSSION

H/D-Ex Analysis of hGHv. The H/D-Ex data clearly identified helix-1 as having different dynamic behavior in hGHv compared to wt-hGH. Of the 15 mutations to the wild-type sequence used to construct hGHv, four are in helix-1: F10A, M14W, H18D, and H21N. The F10A mutation causes large changes in the relative positions of helices-1 and -4, which pack antiparallel with each other (*32*). This residue is an integral part of the packing core and serves as a framework residue, much like framework residues in antibody CDR loops. The removal of the Phe side chain introduces a potential packing void. The molecule responds to this change by a rigid body rotation of ∼12° of helix-1 bringing its N-terminal end closer to helix-4. Concurrently, the C-terminal end of helix-4 moves 1.1 Å closer to helix-1. The space introduced by the absence of the Phe side chain is filled by a water molecule that is totally buried in the hydrophobic core H-bonding to two carbonyl groups, A10 and L177 (*32*).

It is important to note that, while the H/D-Ex data clearly identify that some degree of local unfolding takes place in

helix-1, this phenomenon is not recapitulated in the temperature factor (*B*-factor) data from the X-ray structure of unbound hGHv analyzed at 2.0 Å resolution (PDB code 1HUW). Those data showed no systematic increase in *B*-factors of the main chain atoms in helix-1 compared to those in the other helices in the molecule. This indicates that transient structural fluctuations of significant magnitude can occur in highly "stable" regions of a protein structure which are not reported by time-average-derived parameters such as *B*-factors.

H/D Exchange in the Complex. The binding of the hGHbp to wt-hGH and hGHv introduces a second level of protection against H/D exchange. On the basis of crystallographic evidence, the largest contributor to the Site-1 binding interface on the hormones is helix-4, the middle of helix-1, the mini-helix (residues 38−46), and a short segment of the loop connecting helices-1 and -2 (residues 61−65) (Figure 1). The level of deuteration of wt-hGH and hGHv in their bound complexes is compared in Figure 3b. Here, the hGHv complex shows a slight increase in exchange at residues 12−15, versus wt-hGH, while showing slower exchange at the C-terminal portion of helix-1/mini-helix and a portion of the loop. The latter decrease in exchange in hGHv is likely due to the increased stability of the complex. However, while the exchange properties of the stable complexes are comparable, the changes in the H/D exchange patterns that occur in wt-hGH and hGHv going from their unbound states to their bound ones are substantially different in some areas. The largest changes between the two hormones are in helix-1, the long peptide that includes residues 56−75, and the short peptide between residues 95−97 (Table 1/Figure 4). It is noteworthy that based on structural data, it would be expected that helix-4, which contains the binding hot-spot residues in wt-hGH, would also be identified as being part of the binding interface by this method. However, because helix-4 is very stable and is almost totally resistant to H/D exchange in the unbound molecule, there is no measurable difference in the exchange rates in helix-4 between the unbound and bound states of either wt-hGH or hGHv. Thus, we note an inherent limitation for assigning areas of protein−protein interactions by this method is that the interface residues cannot already be in a low exchange H-bonding environment.

H/D Exchange in the hGHbp. The structure of the hGHbp contains two canonical fibronectin type III domains (FNIII) of about 110 residues connected by a short four-residue linker (*33*). The FNIII domains are organized in a β-sandwich fold consisting of six-stranded β-sheets. The hormones bind to sections of both domains of the hGHbp. The principal binding determinants of the hGHbp are binding loops extending from the β-sheet structure, one in each domain and each containing an essential tryptophan side chain: Trp104 and Trp169.

The H/D exchange characteristics of the unbound and bound forms of the hGHbp are depicted in Figure 5/Table 2. When the hGHbp exchange patterns in the bound forms complexed to wt-hGH and hGHv are compared, it appears that hGHv provides more extensive protection in the interface especially for the binding loop in the second domain containing Trp169 and the linker residues contained in the peptide 123−126.

An interesting and somewhat surprising feature of the H/D exchange pattern for the unbound hGHbp is that moderate exchange occurs in the "buried" β-sheet cores of the FNIII domains (Table 2). From other H/D exchange studies, it has been observed that β-sheet secondary structures are generally more resistant to exchange than α-helices (*12*). This clearly is not the case here where, with the exception of helix-1, the other helices in the four-helix bundle hormones are extremely resistant toward exchange, much more so than the β-sheet NHs in the FNIII domains. However, we believe the most surprising and relevant feature of this analysis of the hGHbp is the difference observed on binding of either hormone in the H/D exchange properties of the β-sheet structures that are not directly involved in binding (Figure 5). What is seen is a rather extraordinary reduction of exchange all over the hGHbp representing a significant "tightening" of the secondary structure throughout the molecule upon binding. Perhaps this stabilization throughout hGHbp (which would likely include additional surface area burial) is also reflected in the larger-than-expected negative ΔC_p values for both wt-hGH and hGHv complexes (*3*). It would seem that binding significantly diminishes the extent of the local breathing motions in the β-strands in the C-terminal domain (residues 154−164 and 196−207), even though they are distant from any contact with the bound hormone. These strands constitute the important stem−stem (hGHbp1-hGHbp2) contact that helps drive the receptor dimerization process (Figure 5d). While there is no direct evidence that this effect plays a role in hGHbp1−hGHbp2 binding and consequent signaling, it is mentioned because the effect is so significant and needs to be further explored.

wt-hGH and hGHv Bind hGHbp Using Different Mechanisms. The H/D exchange and chemical denaturation data indicate the wt-hGH and hGHv display distinctively different dynamic behavior in their unbound states. We believe there is also strong evidence suggesting that the binding of wt-hGH and hGHv differ fundamentally on both thermodynamic and mechanistic levels.

Isothermal titration calorimetry was used to determine the partitioning of the thermodynamic contributions governing the Site-1 binding for both wt-hGH and hGHv (*3*). Those data showed that the wt-hGH interaction exhibited favorable contributions from both ΔH and $-T\Delta S$. On the other hand, in the case of hGHv, the partitioning is very asymmetric; ΔH is highly favorable (−36 kcal/mol) but is counterbalanced by a large unfavorable $-T\Delta S$ term (21 kcal/mol), the latter is about 24 kcal/mol less favorable than that for wt-hGH. The unfavorable ΔS is compensated for by the ΔH contribution that is almost 27 kcal/mol more favorable. Overall, this enthalpically driven equilibrium provides hGHv an additional 3 kcal/mol increase in binding energy. Interestingly, when CD was used to monitor the structural melting as a function of denaturant, it was determined that hGHv is less stable than wt-hGH by about 3 kcal/mol, which perhaps has some implications for its binding mechanism (see below).

The thermodynamic data indicating that the partitioning of ΔH and $T\Delta S$ is radically different between wt-hGH and hGHv along with the stability and H/D exchange data indirectly imply that the mechanisms of binding of these two molecules must, at a level, be quite different. There are two supplementary lines of experimental information that offer more direct evidence for a different binding mechanism.

(i) What Happened to the Binding Hot-Spot? A common trait of protein−protein interactions is that their functional epitopes are characterized by a binding "hot-spot"; a relatively small set of residues, usually spatially focused in a central region, that provide a disproportionally large amount of the total binding energy.

The functional epitope of hGHv was characterized by evaluating the $\Delta\Delta G$ values for 35 alanine mutations of residues that comprise its Site-1 contact interface with the hGHbp (*9*). This analysis identified some rather remarkable differences in its properties compared to the previously determined functional epitope of wt-hGH. Even though hGHv forms a much tighter interaction with hGHbp, overall the so-called "hot-spot" is highly attenuated and the binding contributions of the individual residues appear to be apportioned over a much larger part of the interface. In fact, the hot-spot residues are so attenuated that it is difficult to surmise how hGHv binds as tight as it does. It is also noteworthy that an analogous situation exists with regard to the comparative properties of the hGHbp (Pal and Kossiakoff, unpublished results). hGHbp's binding hot-spot, which is dominated by the loops containing the two essential tryptophans, Trp104 and Trp169, when binding to wt-hGH is similarly attenuated in the case for its binding to hGHv. Additionally, it was also found that some pairwise cooperativity between residues in the hGHbp exists in binding to hGHv, which parallels the binding cooperativity that was observed for hGHv itself. Together, these findings suggest that there is an additional "pool" of binding energy that is available to hGHv through some factors that cannot be identified by classical Ala-scan analysis.

(ii) Differences in Binding Kinetics for the W104A and W169A hGHbp Variants Binding to wt-hGH and hGHv. As mentioned above, for Site-1, the major hGHbp binding determinants are two loops, each containing an essential tryptophan residue. On binding, the tryptophan side chains become deeply buried in the interface and act as essential anchors for productive binding (*7*). Importantly, it has been shown by X-ray structural analysis that the packing of the W104 and W169 side chains in complexes with wt-hGH and hGHv are virtually identical (*5*).

Mutations in hGHbp that remove either of the Trp residues are extremely deleterious to binding of wt-hGH, resulting in a 10 000-fold reduction in the binding constant (*7*). However, for hGHv, the same mutations produce a drastically reduced effect; the W104A and W169A mutants bind with K_d values of 2.3 and 9.2 nM, respectively (∼400−1000-fold reduction in affinity). While it is true that these mutations still have a significant negative impact based on the original affinity of hGHv, it is remarkable that these Trp variants can still bind hGHv with affinities approaching the wild-type molecule. What can be gleaned from this finding is that the binding of wt-hGH has an absolute requirement for the presence of both tryptophans, while for hGHv binding, only W104 is obligatory (*2*).

An additional relevant difference in the binding characteristics of these Trp variants is in their binding kinetics. An almost absolute trait of the many mutations that have been made in the hGH system, both with respect to mutations in the hormone and the hGHbp, is that binding affinities are governed by the off-rate processes (*2*, *3*, *34*). Even the k_{on} rate constants of variants of hGH where 18 nonwild-type substitutions have been made are within a factor of 2 or 3 compared to the wild-type value (*3*). However, in the case of the Trp variants binding to wt-hGH, the k_{on} rates are affected 2−3 orders of magnitude. Surprisingly, these variants bind to hGHv with k_{on} rate constants that are similar (≤ 3-fold) to what has been observed for other mutations. Thus, the energy of the transition state (TS) for wt-hGH binding is 5−6 kcal/mol higher than is the case for hGHv (*2*).

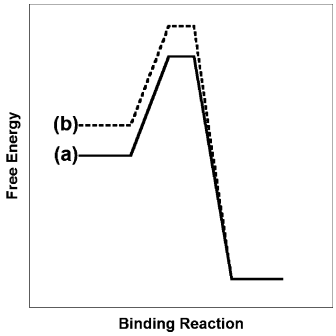

FIGURE 7: Reaction diagram for protein−protein association. Reaction scheme b has elevated initial unbound free energy.

The High Affinity Variant, hGHv, Binds hGHbp by a Different Mechanism. It is difficult to translate the observations above into a consistent conceptual model describing the TS structures of wt-hGH and hGHv binding the Trp variants. Nevertheless, the picture that arises is that the binding of the two hormones differs in some fundamental ways. Consequently, on the basis of these observations and the H/D exchange analysis presented here, we propose that wt-hGH and hGHv bind to the hGHbp through their Site-1 binding site by two distinctly different mechanisms.

Basic binding thermodynamics state that the magnitude for the free energy change upon binding (ΔG_{total}) is determined by the energy difference between the free energy of the unbound state (G_{US}) of the system compared to that of its bound state (G_{BS}). In its simplest form, there are two ways to increase the binding affinity between two molecules: Mechanism 1, lowering the energy of the bound complex (G_{BS}) by forming new energetically favorable interactions, or Mechanism 2, raising the energy of the unbound state (G_{US}) (Figure 7). Of course, a third mechanism could be a hybrid of both, and except for extreme cases, it would be expected that even a binding process that strongly favored one mechanism would still contain a small fraction of the other. Many protein engineering efforts have focused on increasing the affinity between two molecules via Mechanism 1 by introducing optimized electrostatics, H-bonding, and/or van der Waals interactions (*35*−*38*). However, to our knowledge, there are few, if any, that rationally destabilize molecules to improve their binding affinity via the Mechanism 2 pathway. It is important for the case of Mechanism 2 that the factors that destabilize the unbound state do not likewise decrease the stability of the bound state by increasing its energy.

We believe that the stability and H/D exchange data suggest that a mechanism weighted toward Mechanism 2 best explains the 400-fold increase in binding affinity for hGHv. The k_{on} rates for Site-1 binding of hGHv and wt-hGH are very similar, meaning that the energy to reach their

respective TS complexes is also nearly equivalent. However, since hGHv is ~3 kcal/mol less stable than the wild-type molecule, presumably the ground state of the unbound hGHv is also higher in this case. In addition, *m*-value analysis would imply that hGHv exposes less surface area to solvent upon unfolding, suggesting that it is more exposed (less intramolecular buried surface) in the folded, unbound state. Solvent-accessible surface area calculations also show that, when examining the buried intramolecular surface area for the 15 residues that are different between wt-hGH and hGHv, hGHv buries ~200 Å less apolar surface relative to wt-hGH (in its both free and bound states). So, perhaps in too simple terms, an elevation in the ground state energy of the reactants in the hGHv system can explain almost all the increased binding affinity without requiring any lowering of the energy well-defining the energy of the product, the bound hGHv−hGHbp complex. Of course, such a model of a destabilized unbound state would require that the stability of the bound complex and/or the transition state barrier is not adversely affected. An interesting parallel to the example investigated here is work by Stephens and co-workers, where correlations were observed between the extent of reduction in enzyme dynamics upon cofactor binding (as probed by H/D exchange) and cofactor affinity, suggesting dynamics can contribute favorably to binding (*39*). Perhaps these examples highlight the fact that, while changes in dynamics are most commonly attributed to entropic penalties (*40*−*43*), enthalpic contributions should not be overlooked, as they may participate favorably in the transition from the unbound to bound ensembles (*44*).

There are two potential features that allow such a mechanism in the growth hormone system. The first being, as discussed above, that destabilization must not adversely affect the transition state barrier. The highly evolved interface of wt-hGH appears to have been "primed" for recognition, such that the 15-residues substitution in hGHv does not affect the free energy to reach the transition state. Even in its acid-destabilized state as surveyed by NMR, wt-hGH displays dramatically increased dynamics, yet still retains its secondary conformations (*29*), which may be attributed to the 4-helix bundle topology. Second, destabilization in the unbound hGHbp may also play an important role. There is a significant stabilization across hGHbp upon binding both hormones after the transition state is reached. If both proteins (hormone and receptor) require a certain extent of "folding" upon binding, such a mechanism may be used to increase affinity as both proteins are not fully "stable." Such a mechanism, whether both proteins or just one undergoes a "folding" transition upon binding, will be expected to be highly cooperative in nature, largely in terms of its intramolecular interactions.

Finally, perhaps this finding speaks to a more general relationship: the relationship between protein function and fitness. It is clear that a protein's properties, such as catalytic activity or binding affinity, are a product of their environment and evolutionary selection. Gain-of-function mutants have previously been found to decrease enzyme fitness. For example, inhibitors of β-lactamase have selected new β-lactamase mutants capable of new penicillinase activity, but at the price of enzyme thermostability (*45*). Such mutants have also been found to have secondary mutations that restore the lost stability (*45*). With the phage-optimized hGHv (and most typical phage selection strategies) there was no designed selection for a more stable protein; therefore, the energetic landscape that may be explored using such a technique is more extensive. hGHv appears to have made use of this expanded energetic landscape to devise a "nonstandard" mechanism for enhanced affinity. Therefore, as phage display continues to become a more common protein engineering tool, it will be interesting to determine if phage-optimized proteins show a general trend in destabilization and to determine the role such destabilization plays on the selected trait.

CONCLUSIONS

H/D-EX analysis of both wt-hGH and hGHv along with their complexes with hGHbp has allowed insight into the role dynamics play in their molecular recognition. The phage-optimized hGHv's mechanism for enhanced affinity appears to be driven, not by decreasing the free energy of the bound state, but by increasing the free energy of the unbound hormone. In particular, helix-1, a region which contributes significant surface area to the hGHbp interface, is influential in this role. Understanding the differences in the dynamic nature of the two hormones has also helped rationalize the dramatically different binding thermodynamics. Such a structural rationale for hGHv's extremely favorable enthalpy overcoming a very unfavorable entropy has not been revealed through simple crystal structure, spectroscopic data, or biochemical alanine-scanning. This feature most likely exposes the nature of the helix-1 dynamics, whereby side chain fluctuations are dramatic enough to have thermodynamic consequences, yet maintain the same "average" structure. This work may also serve as a model for an emerging class of partially folded (intrinsically unstructured) proteins (*46*, *47*). Future work will help reveal the detailed mechanism of hGHv destabilization and will determine whether such an approach may be applied in a more rational fashion.

ACKNOWLEDGMENT

We thank Mohammed Yousef at the Biophysical Core facility at the University of Chicago for technical assistance with the circular dichroism experiments.

SUPPORTING INFORMATION AVAILABLE

Figures showing peptides used in the analysis of wt-hGH, hGHv, and hGHbp and H/D-Ex results of wt-hGH with or without hGHbp; hGHv with or without hGHbp; wt-hGHv with or without hGHbp; and hGHbp alone an in the presence of wt-hGH or hGHv. This material is available free of charge via the Internet at http://pubs.acs.org.

REFERENCES

1. Lowman, H. B., and Wells, J. A. (1993) Affinity maturation of human growth hormone by monovalent phage display, *J. Mol. Biol. 234*, 564−578.
2. Bernat, B., Sun, M., Dwyer, M., Feldkamp, M., and Kossiakoff, A. A. (2004) Dissecting the binding energy epitope of a high-affinity variant of human growth hormone: cooperative and additive effects from combining mutations from independently selected phage display mutagenesis libraries, *Biochemistry 43*, 6076−6084.

3. Kouadio, J. L., Horn, J. R., Pal, G., and Kossiakoff, A. A. (2005) Shotgun alanine scanning shows that growth hormone can bind productively to its receptor through a drastically minimized interface, *J. Biol. Chem. 280*, 25524−25532.
4. Pearce, K. H., Jr., Cunningham, B. C., Fuh, G., Teeri, T., and Wells, J. A. (1999) Growth hormone binding affinity for its receptor surpasses the requirements for cellular activity, *Biochemistry 38*, 81−89.
5. Schiffer, C., Ultsch, M., Walsh, S., Somers, W., de Vos, A. M., and Kossiakoff, A. (2002) Structure of a phage display-derived variant of human growth hormone complexed to two copies of the extracellular domain of its receptor: evidence for strong structural coupling between receptor binding sites, *J. Mol. Biol. 316*, 277−289.
6. Cunningham, B. C., and Wells, J. A. (1993) Comparison of a structural and a functional epitope, *J. Mol. Biol. 234*, 554−563.
7. Clackson, T., and Wells, J. A. (1995) A hot spot of binding energy in a hormone-receptor interface, *Science 267*, 383−386.
8. Wells, J. A. (1996) Binding in the growth hormone receptor complex, *Proc. Natl. Acad. Sci. U.S.A. 93*, 1−6.
9. Pal, G., Kossiakoff, A. A., and Sidhu, S. S. (2003) The functional binding epitope of a high affinity variant of human growth hormone mapped by shotgun alanine-scanning mutagenesis: insights into the mechanisms responsible for improved affinity, *J. Mol. Biol. 332*, 195−204.
10. Murphy, K. P., and Freire, E. (1992) Thermodynamics of structural stability and cooperative folding behavior in proteins. *Adv. Prot. Chem. 43*, 313−361.
11. Krishna, M. M., Hoang, L., Lin, Y., and Englander, S. W. (2004) Hydrogen exchange methods to study protein folding, *Methods 34*, 51−64.
12. Kossiakoff, A. A. (1982) Protein dynamics investigated by the neutron diffraction-hydrogen exchange technique, *Nature 296*, 713−721.
13. Englander, J. J., Del Mar, C., Li, W., Englander, S. W., Kim, J. S., Stranz, D. D., Hamuro, Y., and Woods, V. L., Jr. (2003) Protein structure change studied by hydrogen−deuterium exchange, functional labeling, and mass spectrometry, *Proc. Natl. Acad. Sci. U.S.A. 100*, 7057−7062.
14. Kossiakoff, A. A. (1985) The application of neutron crystallography to the study of dynamic and hydration properties of proteins, *Annu. Rev. Biochem. 54*, 1195−1227.
15. Hamuro, Y., Coales, S. J., Southern, M. R., Nemeth-Cawley, J. F., Stranz, D. D., and Griffin, P. R. (2003) Rapid analysis of protein structure and dynamics by hydrogen/deuterium exchange mass spectrometry, *J. Biomol. Tech. 14*, 171−182.
16. Zhang, Z., and Smith, D. L. (1993) Determination of amide hydrogen exchange by mass spectrometry: a new tool for protein structure elucidation, *Protein Sci. 2*, 522−531.
17. Resing, K. A., Hoofnagle, A. N., and Ahn, N. G. (1999) Modeling deuterium exchange behavior of ERK2 using pepsin mapping to probe secondary structure, *J. Am. Soc. Mass Spectrom. 10*, 685−702.
18. Neubert, T. A., Walsh, K. A., Hurley, J. B., and Johnson, R. S. (1997) Monitoring calcium-induced conformational changes in recoverin by electrospray mass spectrometry, *Protein Sci. 6*, 843−850.
19. Engen, J. R., and Smith, D. L. (2001) Investigating protein structure and dynamics by hydrogen exchange MS. *Anal. Chem. 73*, 256A−265A.
20. Hoofnagle, A. N., Resing, K. A., Goldsmith, E. J., and Ahn, N. G. (2001) Changes in protein conformational mobility upon activation of extracellular regulated protein kinase-2 as detected by hydrogen exchange, *Proc. Natl. Acad. Sci. U.S.A. 98*, 956−961.
21. Engen, J. R., Gmeiner, W. H., Smithgall, T. E., and Smith, D. L. (1999) Hydrogen exchange shows peptide binding stabilizes motions in Hck SH2, *Biochemistry 38*, 8926−8935.
22. Andersen, M. D., Shaffer, J., Jennings, P. A., and Adams, J. A. (2001) Structural characterization of protein kinase A as a function of nucleotide binding. Hydrogen−deuterium exchange studies using matrix-assisted laser desorption ionization-time of flight mass spectrometry detection, *J. Biol. Chem. 276*, 14204−14211.
23. Burns-Hamuro, L., Hamuro, Y., Kim, J., Sigala, P., Fayos, R., Stranz, D., Jennings, P., Taylor, S., and Woods, V. J. (2005) Distinct interaction modes of an AKAP bound to two regulatory subunit isoforms of protein kinase A revealed by amide hydrogen/deuterium exchange, *Protein Sci. 14*, 2982−2992.
24. Baerga-Ortiz, A., Bergqvist, S., Mandell, J., and Komives, E. (2004) Two different proteins that compete for binding to thrombin have opposite kinetic and thermodynamic profiles, *Protein Sci. 13*, 166−176.
25. Hamuro, Y., Anand, G., Kim, J., Juliano, C., Stranz, D., Taylor, S., and Woods, V. J. (2004) Mapping intersubunit interactions of the regulatory subunit (RIalpha) in the type I holoenzyme of protein kinase A by amide hydrogen/deuterium exchange mass spectrometry (DXMS), *J. Mol. Biol. 340*, 1185−1196.
26. Chang, C. N., Rey, M., Bochner, B., Heyneker, H., and Gray, G. (1987) High-level secretion of human growth hormone by *Escherichia coli*, *Gene 55*, 189−196.
27. Fuh, G., Mulkerrin, M. G., Bass, S., McFarland, N., Brochier, M., Bourell, J. H., Light, D. R., and Wells, J. A. (1990) The human growth hormone receptor. Secretion from *Escherichia coli* and disulfide bonding pattern of the extracellular binding domain, *J. Biol. Chem. 265*, 3111−3115.
28. Hubbard, S. J., and Thornton, J. M. (1993) Department of Biochemistry and Molecular Biology, University College London, U.K.
29. Kasimova, M. R., Kristensen, S. M., Howe, P. W., Christensen, T., Matthiesen, F., Petersen, J., Sorensen, H. H., and Led, J. J. (2002) NMR studies of the backbone flexibility and structure of human growth hormone: a comparison of high and low pH conformations, *J. Mol. Biol. 318*, 679−695.
30. Clackson, T., Ultsch, M. H., Wells, J. A., and de Vos, A. M. (1998) Structural and functional analysis of the 1:1 growth hormone: receptor complex reveals the molecular basis for receptor affinity, *J. Mol. Biol. 277*, 1111−1128.
31. Myers, J. K., Pace, C. N., and Scholtz, J. M. (1995) Denaturant m values and heat capacity changes: relation to changes in accessible surface areas of protein unfolding, *Protein Sci. 4*, 2138−2148.
32. Ultsch, M. H., Somers, W., Kossiakoff, A. A., and de Vos, A. M. (1994) The crystal structure of affinity-matured human growth hormone at 2 Å resolution. *J. Mol. Biol. 236*, 286−299.
33. de Vos, A. M., Ultsch, M., and Kossiakoff, A. A. (1992) Human growth hormone and extracellular domain of its receptor: crystal structure of the complex, *Science 255*, 306−312.
34. Walsh, S. T., Jevitts, L. M., Sylvester, J. E., and Kossiakoff, A. A. (2003) Site2 binding energetics of the regulatory step of growth hormone-induced receptor homodimerization, *Protein Sci. 12*, 1960−1970.
35. Marvin, J. S., and Lowman, H. B. (2003) Redesigning an antibody fragment for faster association with its antigen, *Biochemistry 42*, 7077−7083.
36. Baca, M., Scanlan, T. S., Stephenson, R. C., and Wells, J. A. (1997) Phage display of a catalytic antibody to optimize affinity for transition-state analog binding, *Proc. Natl. Acad. Sci. U.S.A. 94*, 10063−10068.
37. Schreiber, G., and Fersht, A. R. (1996) Rapid, electrostatically assisted association of proteins, *Nat. Struct. Biol. 3*, 427−431.
38. Selzer, T., Albeck, S., and Schreiber, G. (2000) Rational design of faster associating and tighter binding protein complexes, *Nat. Struct. Biol. 7*, 537−541.
39. Williams, D. H., Zhou, M., and Stephens, E. (2006) Ligand binding energy and enzyme efficiency from reductions in protein dynamics, *J. Mol. Biol. 355*, 760−767.
40. Kovrigin, E. L., Cole, R., and Loria, J. P. (2003) Temperature dependence of the backbone dynamics of ribonuclease A in the ground state and bound to the inhibitor 5′-phosphothymidine (3′-5′)pyrophosphate adenosine 3′-phosphate, *Biochemistry 42*, 5279−5291.
41. Spyracopoulos, L., and Sykes, B. D. (2001) Thermodynamic insights into proteins from NMR spin relaxation studies, *Curr. Opin. Struct. Biol. 11*, 555−559.
42. Wang, C., Pawley, N. H., and Nicholson, L. K. (2001) The role of backbone motions in ligand binding to the c-Src SH3 domain, *J. Mol. Biol. 313*, 873−887.
43. Lee, A. L., Kinnear, S. A., and Wand, A. J. (2000) Redistribution and loss of side chain entropy upon formation of a calmodulin-peptide complex, *Nat. Struct. Biol. 7*, 72−77.
44. Horn, J. R., Ramaswamy, S., and Murphy, K. P. (2003) Structure and energetics of protein−protein interactions: the role of conformational heterogeneity in OMTKY3 binding to serine proteases, *J. Mol. Biol. 331*, 497−508.

45. Wang, X., Minasov, G., and Shoichet, B. K. (2002) Evolution of an antibiotic resistance enzyme constrained by stability and activity Trade-offs, *J. Mol. Biol. 320*, 85−95.
46. Wright, P. E., and Dyson, H. J. (1999) Intrinsically unstructured proteins: re-assessing the protein structure−function paradigm, *J. Mol. Biol. 293*, 321−331.
47. Dyson, H. J., and Wright, P. E. (2005) Intrinsically unstructured proteins and their functions, *Nat. Rev. Mol. Cell Biol. 6*, 197−208.
48. DeLano, W. L. (2002), DeLano Scientific, San Carlos, CA.

BI0604328